Chemical Methodologies 6(2022) 823-830

Chemical Methodologies

Journal homepage: http://chemmethod.com

Original Research Article

Synthesis of Carbon Quantum Dot by Electro-Chemical Method and Studying Optical, Electrical, and Structural Properties

Ahmed Hamid Abd*, Omar Adnan Ibrahim

Department of physics, College of Science, University of Baghdad, Iraq

ARTICLE INFO

Article history

Submitted: 2022-05-13
Revised: 2022-06-22
Accepted: 2022-07-27
Manuscript ID: CHEMM-2207-1575
Checked for Plagiarism: **Yes**
Language Editor:
Dr. Fatimah Ramezani
Editor who approved publication:
Professor Dr. Hassan Karimi-Maleh

DOI:10.22034/CHEMM.2022.351559.1575

KEYWORDS

Carbon quantum dots (CQDs)
UV
LEDs
XRD

ABSTRACT

Carbon quantum dot light is produced by the UV-lit nanoparticles (NPs), and LEDs are explained. They created the nanoparticles. The Poisson equation was used to forecast surface state levels that surface nanostructure would cause to emerge in the optical energy spectrum of CQDs. The chromaticity of the produced light coordinates and the wavelength of the associated color was determined by using the photoluminescence (PL) spectrum. A study of the X-ray diffraction (XRD) was carried out to determine the type of material and size.

GRAPHICAL ABSTRACT

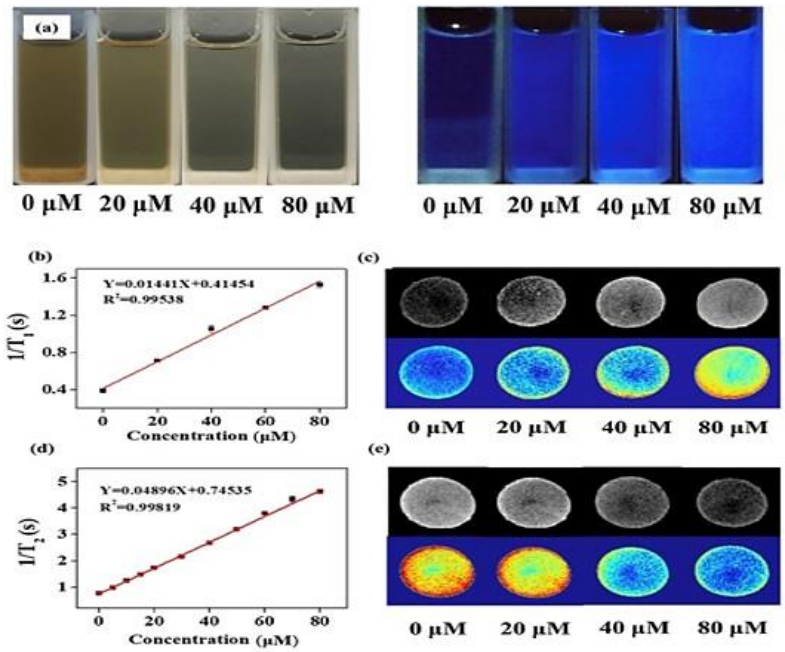

* Corresponding author: Ahmed Hamid Abd
✉ E-mail: Forat. ahmed.hameed1204a@sc.uobaghdad.edu.iq

Introduction

Because lighting accounts for 25% of global electricity usage, light generation has sparked a considerable attention as a means of reducing electrical energy consumption and hence operational costs [1]. Many strategies have been reported to generate light [2, 3]. To make light, one of the most common methods is to mix red, green, and blue phosphor in a proper ratio [4, 5]. This is significant not only because of the financial rewards, but also because the SSL is expected to significantly cut carbon emissions, resulting in a cleaner environment. When it comes to converting energy to light, SSL is 50% efficient compared to around 1% for standard lamps. Furthermore, SSL offers ultra-long bulb lifetimes, and the source becomes ragged and compact.

Because of their potential for using in solid-state lighting, nanoluminophors are of high significance. Semiconductors such as CQDs, CdSe, ZnS, and ZnSe with sizes ranging from 1 to 10 nm are commonly employed in nanoluminophors [6]. The features of the surface atoms have a profound influence on the materials. Because the nanostructure comprises a greater more surface atoms than in the interior, it has significant physical and chemical characteristics.

Since trap-states can be found in surface states, the primary energy gap of nano semiconductor when illuminated by the UV light, they emit radiation with high quantum efficiency [7]. The emission from rich in traps nanocrystals is far more beneficial than that of doped-semiconductor nanocrystals. As a result of their collective emission in blue from CQDs and yellow from the Mn d-d level, the Mn-doped nanocrystal produces light. The quantum efficiency of the emitted light, on the other hand, is extremely poor [7, 8]. Chemical synthesis is used to make CQDs NCs quantum dots in this study. The white light is generated with high efficiency by NCs with trap-rich CQDs lit by a GaN UV-LED. A hybrid nanoparticles light emitting diode (NPs-LED) was fabricated as layers of ITO/TPD:PMMA/Eu_2O_3/Alq_3/Al by phase segregation method via spin coating technique [9].

Materials and Methods

Preparation of colloidal CQDs nanoparticle

All materials NaOH, C_2H_5OH, and PMMA were purchased from Merck and they were while stirring with a magnetic stirrer, and then this mixture was left on a magnetic stirrer for 15 minutes to completely dissolve the (NaOH). The solution was transferred to the next graphite rod positionnext, it was poured into a 250 mL beaker while connected to a power source. One-inch rods were immersed in the solution and the carbon rods were separated. The distance between both electrodes is approximately 2 cm. The electrodes were flipped each 5 minute to transport ions from one electrode to the next. After that, the resultant solution was poured into the vial labels and they were shut. The solution was left for 5 days. The color was yellow-orange, as it turned out. In addition to other methods for preparing CQDs, it was prepared by a pulsed laser ablation, but the electrochemical method is the best one [10].

Preparation of a CQDs/PMMA composite film

Before explaining the fabrication method of light generation device, one should know the reasons for choosing PMMA and CQDs. The CQDs were chosen because they contain the majority of native defects that induce deep levels emission (DLE) at various locations in the band gap, allowing for observing a sizable number of luminescence lines of various energies. This explains why different CQDs NPs samples have experimentally revealed to exhibit all of the visible hues. Blue luminescence, green luminescence, and red luminescence DLE bands are most often seen bands in CQDs, and these devices may be utilized to produce light. As a host matrix for the CQDs, polymethyl methacrylate (PMMA) was used, and it offers a transparent host matrix for our organic-inorganic hybrid film.

The (PMMA) solutions were prepared by dissolving from each 70 mg/mL in the chloroform, the mixture (PMMA: CQDs) ratio was taken as (1 mlL10 wt%). The mixture was created by taking 1 mL of (PMMA) and 10 %wt ratio was added from CQDs, and then it was stirred for 15 minutes with a magnetic stirrer at heating to 50 °C before being

placed in a flat-bottomed petri dish to produce an 8 mm-thick film having a strong focus of 13.8 mmol/mL. This approach was created for different concentrations, including 50, 70, and 90.

Testing of the samples that have been prepared

X-Ray diffraction

The SHIMADZU XRD-6000 was used to record the CQDs nanoparticle powder X-ray diffraction (XRD) pattern. A (CuK radiation line with a wavelength of 1.54 A in the wavelength range of 5 to 60 is used in the X-ray diffractometer. Figure 1 displays that the prepared CQDs have polycrystalline structure. The X-ray diffraction patterns include many diffraction peaks and a strong orientation peak at 2θ = 33° which belongs to (004) diffraction line ndicating the XRD spectra of the synthesized CQDs particles under different reaction. All peaks in the XRD spectra could be seen on the standard card of anatase which confirms that the prepared CQDs are an anatase type. Anatase is more favorable for the photocatalytic reaction due to more defects in the crystal lattice to improve the separate of electrons and holes. As the reaction time increases, the intensity of each crystal plane diffraction peak increases gradually and the peak width becomes narrower at half a height.

Absorption and PL spectra

The UV-V of the samples is absorption spectra obtained by using an (SHIMADZU/ origin Japan) UV/VIS spectrophotometer in the wavelength range of 1800 nm. With the use of an SL 174 spectrofluorometer, the photoluminescence spectrum (PL) was recorded, which covered a wavelength range of (300–900) nm. To create the light, (GaN UV-LED) with 5 mW of electricity was used to illuminate the CQDs/PMMA composite films.

From absorption spectrum, the peak at 290 nm which is absent for the lower V.B to upper C.B, and the emission spectrum of CQDs excited by 290 nm wavelength is illustrated in Figure 2. The emission peaks red shift when increase the time reaction, that means the crystal size increases when increases the reaction time that is compatible with Brus equation [11].

The energy gap forms are the peaks of emission spectrum for CQDs were calculated by using Planck equation and found to be 3.1eV. The QDs size (29nm) was calculated from Brus equation (1) [11]:

$$Eg_{QDs} = Eg_{bulk} + \frac{\hbar^2\pi^2}{2ed^2m_o}\left(\frac{1}{m_e}+\frac{1}{m_h}\right) - \frac{1.8e}{4\pi\varepsilon\varepsilon_o d} \qquad (1)$$

Where EgQDs is the QDs band gap (=3.1), Egbulk bulk band gap is (5.4ev), the electron's effective mass is me. (= 0.030), m_h is the hole effective mass (=0.035), e is the electron charge (1.6 x 10^{-19}Col), d is the Size of QDs, m_0 is the free electron mass (9.1x10^{-31}kg), ε_o is the permittivity of free space (8.854 x 10^{-12} F/m), and ε_r is the relative permittivity (31).

Where it turns out that the size of the crystal according to Brus equation (57). Its comparison with the size SEM (54) will be a mixed result.

The energy bandgap was calculated from the absorption spectrum by using the graph displayed in Figure 3. Extrapolating the padded portion of (αhυ) 2 against the energy of the photon (hυ) gives an energy band gap of about 3.1 eV for concentrations. The value of this energy gap was completely comparable with the theoretical value given in the literature [12].

Results and Discussion

As previously mentioned, the result CQDs nanoparticles were XRD examined by using a k Cu source line with a wavelength of 1.54 A.

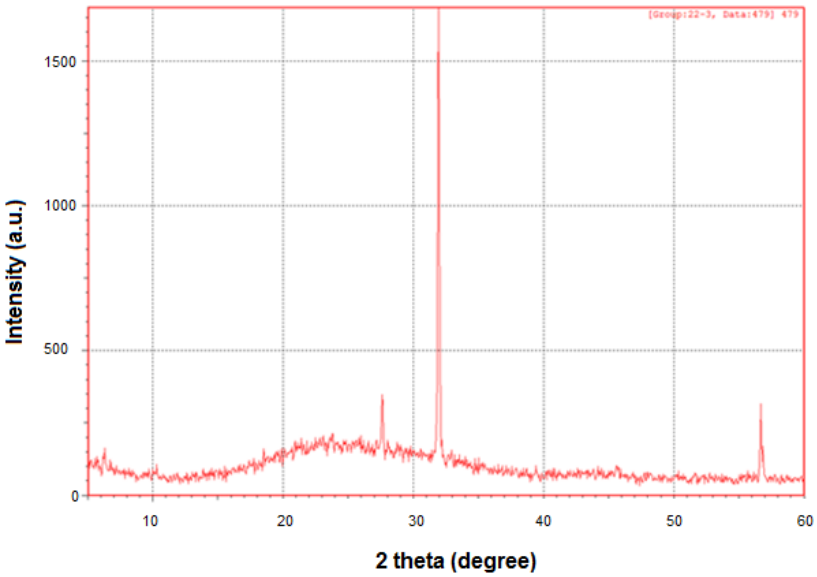

Figure 1: The CQDs sample of X-Ray diffraction pattern

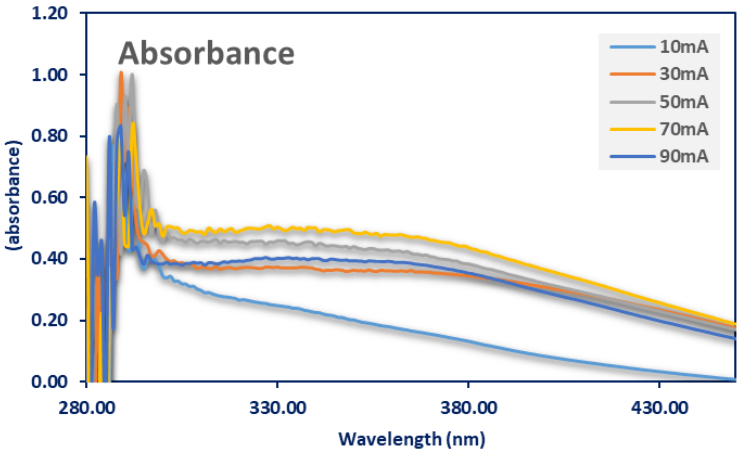

Figure 2: The UV-Vis absorption spectra of the CQDs nanoparticles

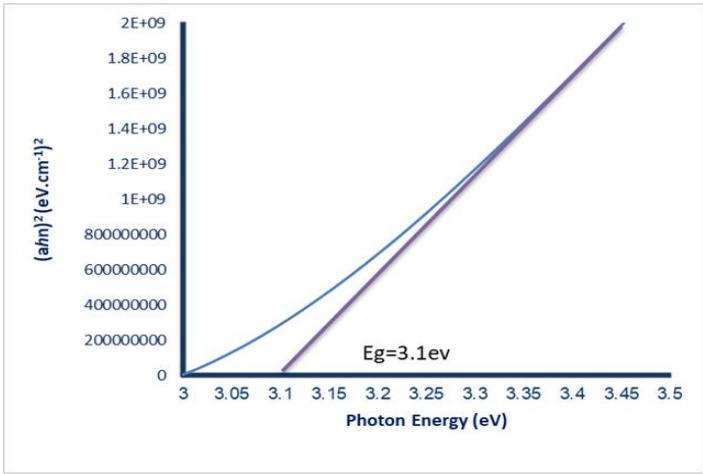

Figure 3: $(\alpha h\upsilon)^2$ vs. photon energy for CQDs film concentration

Figure 1 depicts the XRD pattern. The significant peaks can be seen in the graph, indicating that the nanostructure has been formed. Making the use of the breadth of the (111), which appears from an angle 32 on 2 and take advantage of another view (022) which appears from angle 27 on the scale 2. The peak in the Scherer relation is calculated as follow [13]:

$$D = 0.9\,\lambda/\beta COS\theta$$

The generated nanoparticles had a size of around 29 nm, D is the grain size, W is the wavelength, in degrees is the full width at half maximum (FWHM), and D is the diffraction angle.

As depicted in Figure 4, the device is used in an optical emission spectrometer wavelength range of (340–740) nm. The spectrum shows a peak at 550 nm which can be referred to the direct band transition and which is attributed to the formation of surface states in the energy gap. The emergence of distinct PL spectrum peaks can be identified in relation to the dimension of nanostructures in the above range in the PL spectrum.

With the above parameters mentioned, Figure 4 displays surface states or mid-gap trap states. The emission generated by the transitional region between the (CB) and mid-gap surface states was about 450, 550, and 650 nm, as illustrated in Figure 5.

The CQDs nanocrystals were scattered across a (PMMA) matrix, which was illuminated by a GaN UV-LED to induce a wide smearing-state emission throughout the whole observable range, resulting in different colors, as demonstrated in Figure 6**a**.

Color temperature correlations and chromaticity coordinates (CCT)

A LED's or other source of light's general illumination in the light source should have an acceptable color temperature to correctly depict all colors of lit objects. The XYZ color matching functions weight a certain light's spectrum [14]. Since the CIE colorimetry method expresses the color of light. the area is found under the curve for the three peaks in red, green, and blue centered at 450, 550, and 650 nm to obtain three weighted X, Y, and Z integral values. On the CIE colorimetry system, the chromaticity coordinates x and y are determined as follow:

$$x = X/(X + Y + Z)$$

$$y = Y/(X + Y + Z)$$

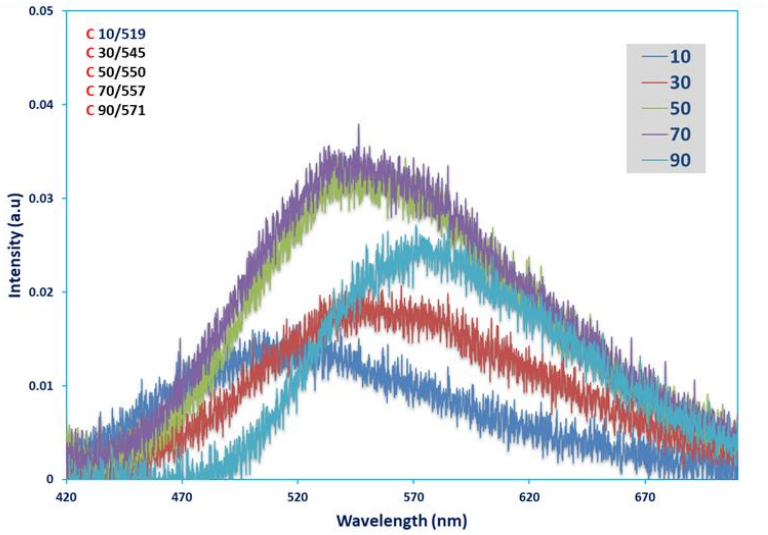

Figure 4: Photoluminescence (PL) emission spectrum of CQDs nanoparticle

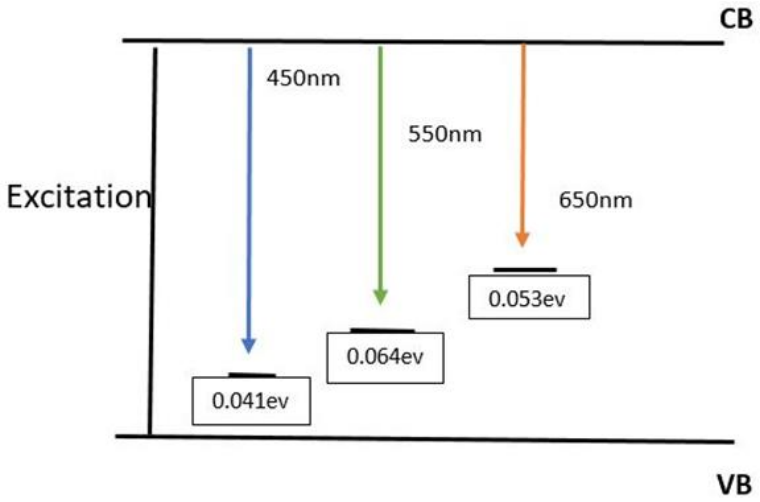

Figure 5: The mid-gap trap status of the CB-Trap state transition

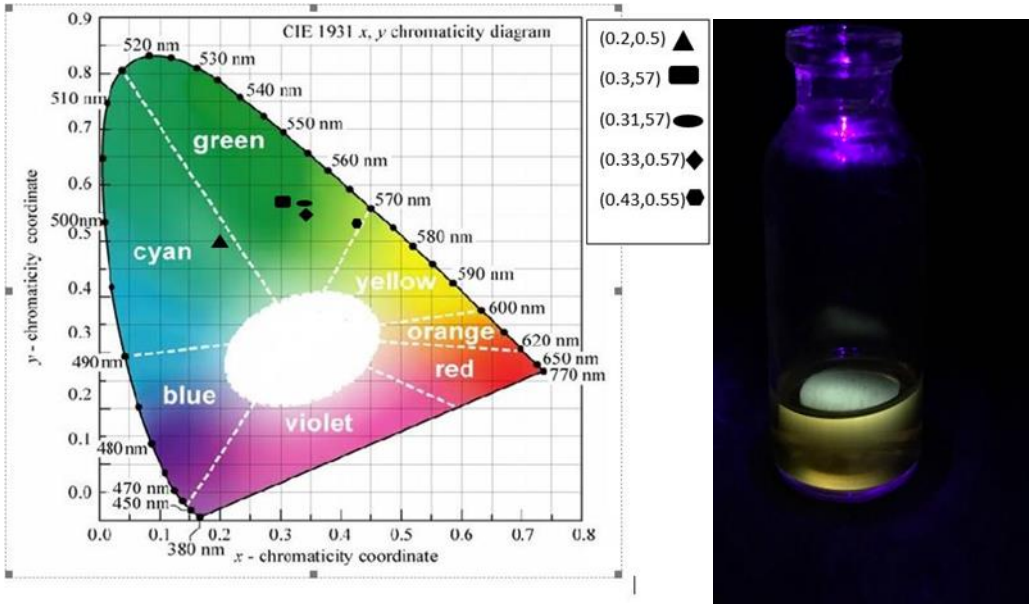

Figure 6: a) CQDs nanoparticle tristimulus coordinates (0.33, 0.56) on the CIE 1931 chromaticity diagram, b) A snapshot of light production from a GaN UV-LED-illuminated CQDs/PMMA composite film

Table 1: Calculate the points for X and Y

X	Y
0.2	0.5
0.33	0.56
0.31	0.57
0.3	0.57
0.43	0.55

The area under the curve of the emitted red, green, and blue in the PL spectrum is X, Y, and Z, correspondingly.

The chromaticity coordinate (x, y) on the CIE 1931 (x, y) chromaticity diagram can be used to express any hue light. The tristimulus coordinates of the green light produced by our CQD nanoparticles are (x, y) = (0.2, 0.5) (Table 1). For the rest of the points, see Figure 6a above. Via McCamy's approximation method to get the CCT from the xy chromaticities, the correlated color temperature (CCT) can be verified for the generated light [14]:

$$CCT=-449n3+3525n2-6823.3n+5520.33 \quad (5)$$

Where,

$$n=\frac{x-0.3320}{y-0.1858}$$

The light's color temperature when it is produced was discovered by using the previously

determined x and y values, as indicated in the following Table 2.

Table 2: The color temperatures of CQDs

Current change	CCT
10 mA	3300 K
30 mA	5500 K
50 mA	5200 K
70 mA	5000 K
90 mA	4000 K

The output light of the emission lines found in the PL spectrum is in the light region, as displayed in Figure 6**a**, which was corroborated by a light snapshot generated by the (CQDs/PMMA) film composite lighted by a (GaN UV-LED), as seen in Figure 6**b**.

Conclusion

The GaN UV-LED irradiation of CQDs NCs (with an average wavelength of 6 nm) resulted in light emission. Peaks in the PL spectra of CQDs NCs are the result of surface-state transitions and the direct band transitions. The green light is produced by CQDs NCs illuminated by the UV-LEDs by using (0.33, 0.56) chromaticity coordinates which is within the green section of the CIE 1931 diagram. These NCs indicate a blue shift in its absorption spectra. The wavelength is 35 nanometers. There seems to be no change in emissions as a result of the study of samples spectroscopy in solution and the solid state.

Acknowledgments

Thanks, and all friends that helped me in this work also thank the Department of Physics in the College of Science/University Baghdad.

Funding

This research did not receive any specific grant from funding agencies in the public, commercial, or not-for-profit sectors.

Authors' contributions

All authors contributed to data analysis, drafting, and revising of the paper and agreed to be responsible for all the aspects of this work.

Conflict of Interest

There are no conflicts of interest in this study.

ORCID:

Ahmed Hamid Abd
https://www.orcid.org/0000-0002-1077-7556

References

[1]. Suhail A.M., Khalifa M.J., Saeed N.M., Ibrahim O.A., White light generation from CdS nanoparticles illuminated by UV-LED, *The European Physical Journal Applied Physics*, 2010, **49**:30601 [Crossref], [Google Scholar], [Publisher]

[2]. Zhao B., Zhang H., Miao Y., Wang Z., Gao L., Wang H., Hao Y., Li W., High color stability and CRI (> 80) fluorescent white organic light-emitting diode based pure emission of exciplexes by employing merely complementary colors, *Journal of Materials Chemistry C*, 2018, **6**:304 [Crossref], [Google Scholar], [Publisher]

[3]. Zhu S., Meng Q., Wang L., Zhang J., Song Y., Jin H., Zhang K., Sun H., Wang H., Yang B., Highly photoluminescent carbon dots for multicolor patterning, sensors, and bioimaging, *Angewandte Chemie International Edition*, 2013, **52**:3953 [Crossref], [Google Scholar], [Publisher]

[4]. Kumar B.G., Sadeghi S., Melikov R., Aria M.M., Jalali H.B., Ow-Yang C.W., Nizamoglu S., Structural control of InP/ZnS core/shell quantum dots enables high-quality white LEDs, *Nanotechnology,* 2018, **29**:345605 [Crossref], [Google Scholar], [Publisher]

[5]. Sadeghi S., Bahmani Jalali H., Melikov R., Ganesh Kumar B., Mohammadi Aria M., Ow-Yang C.W., Nizamoglu S., Stokes-shift-engineered indium phosphide quantum dots for efficient luminescent solar concentrators. *ACS applied materials & interfaces*, 2018, **10**:12975 [Crossref], [Google Scholar], [Publisher]

[6]. Yuan M., Liu M., Sargent E.H., Colloidal quantum dot solids for solution-processed solar cells, *Nature Energy*, 2016, **1**:1 [Crossref], [Google Scholar], [Publisher]

[7]. Lee J., Yang J., Kwon S.G., Hyeon T., Nonclassical nucleation and growth of inorganic nanoparticles, *Nature Reviews Materials*, 2016, **1**:1 [Crossref], [Google Scholar], [Publisher]

[8]. Su L., Zhang X., Zhang Y., Rogach A.L., Recent progress in quantum dot based white light-emitting devices, *Photoactive semiconductor nanocrystal quantum dots*, 2017, 123-147. [Crossref], [Google Scholar], [Publisher]

[9]. Mohammed H.R., Ibrahim O.A., Electroluminescence of Light-Emitting Organic Semiconductor/Europium Oxide Nanoparticle Hybrid Junction, *Iraqi Journal of Science*, 2020, **61**:1952 [Crossref], [Google Scholar], [Publisher]

[10]. Addie A., Khashaan K.S., Saimon J., Hassan A., Impact of Laser Energy on Features of Carbon Nanostructure Materials Prepared by A One-Step Pulsed Laser Ablation in Water, *Iraqi Journal of Science*, 2021, **7**:2197 [Crossref], [Google Scholar], [Publisher]

[11]. Brus L.E., Electron–electron and electron-hole interactions in small semiconductor crystallites: The size dependence of the lowest excited electronic state. *The Journal of chemical physics*, 1984, **80**:4403 [Crossref], [Google Scholar], [Publisher]

[12]. Hussein N.L., Khashan K.S., Rasheed H.M., Hammoud H.Y., ALHaddad R.M., Simulation of Optical Energy Gap for Synthesis Carbon Quantum Dot by Laser Ablation, *Iraqi Journal of Science*, 2019, 52 [Google Scholar], [Publisher]

[13]. Melikov R., Press D.A., Ganesh Kumar B., Sadeghi S., Nizamoglu S., Unravelling radiative energy transfer in solid-state lighting, *Journal of Applied Physics*, 2018, **123**:023103 [Crossref], [Google Scholar], [Publisher]

[14]. Li X., Wang Z., Liu Y., Zhang W., Zhu C., Meng X., Bright tricolor ultrabroad-band emission carbon dots for white light-emitting diodes with a 96.5 high color rendering index, *Journal of Materials Chemistry C*, 2020, **8**:1286 [Crossref], [Google Scholar], [Publisher]

HOW TO CITE THIS ARTICLE

Ahmed Hamid Abd, Omar Adnan Ibrahim. Synthesis of carbon quantum dot by electro-chemical method and studying optical, electrical, and structural properties. *Chem. Methodol.*, 2022, 6(11) 823-830
https://doi.org/10.22034/CHEMM.2022.351559.1575
URL: http://www.chemmethod.com/article_154431.html